Neoclassical Approach to Angular Momentum Transport and Toroidal Rotation in Tokamak Plasmas

C. Yarım 1), U. Daybelge 1), and A. Nicolai 2)

1) Istanbul Technical University, Dept. of Astronautical Eng., Maslak/Istanbul, TURKEY
2) Institut für Plasmaphysik, Forschungszentrum Juelich, Association EURATOM-FZJ, Trilateral Euregio Cluster, D-52425, Juelich, GERMANY

E-mail contact of main author: yarim@itu.edu.tr

Abstract. Approaching the problem of toroidal momentum evolution within the framework of the neoclassical theory with the corrected Braginskii stress tensors, this paper looks for the counterparts of terms like fluxes and sources in the momentum conservation equations and presents their numerical solutions for the evolution of the toroidal and poloidal velocities. Present study considers a subsonic, collisional plasma in front of the magnetic separatrix having a model temperature profile with a controllable gradient and a pedestal height. Study indicates a nonlinear, two-time-scales-coupling between the poloidal and toroidal rotation velocities and shows that the poloidal rotation velocity has a faster response time. If gyrostress tensor is properly taken into account, however; the longer-time evolution of the poloidal and toroidal rotation velocities are strongly coupled. This behaviour is found to be governed by a system of three quasilinear partial differential equations where the space variable is a radial boundary layer distance from the magnetic separatrix. Possibility of a solution is determined by the chosen initial and boundary conditions, (Dirichlet or Neumann), at both limits of the radial boundary layer and the gradient and pedestal height of the model temperature curve used. Steep temperature gradients are found to lead to rapidly diverging rotation velocity profiles.

1. Introduction

Rotation profiles have an important role in the self-regulating mechanisms related to the transition to the better confinement modes of tokamak plasmas [1]. Former interest for the explanation of the observed poloidal plasma rotation in tokamaks [2-4], has lately shifted to the analysis of spontaneous toroidal rotation [1, 5-8], since it does not require an external momentum driver, which may not be available in the future large devices such as ITER [1]. Self-generated toroidal rotation has been observed in many tokamaks, mostly in co-current direction at the edge [1, 9], whereas some counter-current rotation is also observed with strong negative electric field in recent experiments for different heating methods [10].

The plasma rotation problem can be formulated as a conservation equation for the toroidal momentum, deriving the flux and source terms of the toroidal momentum and the convection velocity arising, for example, from various turbulence mechanisms [7]:

$$m_i N_i R \frac{\partial V_\phi}{\partial t} = -\nabla \cdot \left[m_i N_i R \left(\chi_\phi \frac{\partial V_\phi}{\partial r} + V_{pinch} V_\phi \right) + \Pi_{res} \right] + \eta \,, \qquad (1)$$

where m_i is the ion mass, N_i is the ion density, R is the major radius, V_φ is the toroidal velocity, χ_φ is the effective diffusivity, V_{pinch} is the convective velocity, Π_{res} is the residual stress and η is the possible external torque. Note that the convective derivative term on the right hand side has dropped out in the surface averaging of equation (1) [11].

This paper looks for the counterparts of various terms in equation (1) in the regime of high collisionality and presents numerical solutions for the evolution of the toroidal and poloidal velocities assuming a model temperature profile with a controllable gradient and a pedestal

height. In the second section, basic equations describing the plasma at the collisional edge region of a tokamak plasma, and the adopted temperature distribution have been introduced. In the third section an outline of a numerical solution procedure for these equations and in the fourth section the results have been given. Discussion of the results and the conclusion are in the fifth section.

2. Governing equations

It has been shown [12] that a collisional model of plasma at the edge region of tokamak plasmas near the magnetic separatrix is consistent with a series of past experiments. For example, in some shots of Alcator C-Mod ELM-free Ohmic discharges and both L- and H-modes of ASDEX-U device near the edge region the non-dimensional collision frequency is $\hat{\nu} = qR\nu_i / c_i >> 0.222$, indicating that the plasma is collisional [13], where q is the safety factor, ν_i is the ion-ion collision frequency, and c_i is the thermal speed of ions. In this study we approach the problem of toroidal and poloidal rotation of plasmas in the context of the revisited neoclassical theory [14-18] accounting the effects of steep temperature and density profiles where the standard neoclassical theories would not be adequate.

The equations of toroidal momentum evolution within the framework of revisited neoclassical theory [14], including the corrections [19] to the stress tensors in the Braginskii's two-fluid equations [20], have already been obtained for the edge region of tokamak devices with circular [15] and arbitrary [16] cross-sections including various source terms [17] in subsonic region. Flux surface averaged equation for circular cross section tokamak is:

$$m_i N_i \frac{\partial U_{\varphi,i}}{\partial t} = \frac{\partial}{\partial r}\left[\eta_{2,i}\left(\frac{\partial U_{\varphi,i}}{\partial r} - \frac{0.107 q^2}{1+Q^2/S^2}\frac{\partial \ln T_i}{\partial r}\frac{B_\varphi}{B_\theta}U_{\theta,i}\right)\right] + J_r B_\theta - m_i \oint \frac{d\vartheta}{2\pi} h^2 S_i^N U_{\varphi,i} + \oint \frac{d\vartheta}{2\pi} h^2 \vec{S}_i^M \cdot \vec{e}_\varphi \quad (2)$$

where U_θ and U_φ are the poloidal and toroidal velocities. r is the minor radius. J_r is the radial polarization current. and are possible externally applied particle and momentum sources, such as charge exchange and neutral beam injection. $Q = [4B_\varphi U_{\theta,i} - 2.5(T_i / e_i)\partial \ln N_i^2 T_i / \partial r]B^{-1}$, and $S = 2r\chi_{\|,i} N_i^{-1} / (q^2 R^2)$, parallel heat diffusion coefficient is $\chi_{\|,i} = 3.9 P_i / m_i \nu_i$. B, B_θ and B_φ are the total, poloidal and toroidal magnetic fields, respectively. $\eta_{2,i}$ is the perpendicular viscosity coefficient. is the unit vector in toroidal direction and $h = [1 + (r/R)\,\mathrm{Cos}\theta]$.

The second term in the right-hand side of equation (2) has originated from the gyrostress tensor. It provides toroidal torque even when there is no external toroidal momentum source, such as imparted by a neutral beam injection [16].

By using a similar approach, the flux-surface averaged equation of the poloidal motion for both arbitrary and circular cross-section of tokamak plasmas in the edge region can be obtained [16] and extended to include faster time-scales [17]. Flux surface averaged parallel momentum equation for circular cross section tokamak is:

$$m_i N_i (1+2q^2)\partial_t U_{\theta,i} = q^2 \varepsilon^{-1} m_i < \tilde{Z}\cos\theta > U_{\theta,i} + < S^M_{\theta,i} >$$

$$-\frac{3\eta_{0,i}}{2R^2}\left(U_{\theta,i} + \frac{1.833}{e_i B_\varphi}\frac{\partial T_i}{\partial r}\right) + 0.54\frac{\eta_{2,i}\, q^2}{1+Q^2/S^2}\frac{e_i B_\varphi}{T_i}\frac{\partial \ln T_i}{\partial r}\left[\frac{T_i}{e_i B_\theta}\frac{\partial U_{\varphi,i}}{\partial r} + \frac{1}{2}U^2_{\varphi,i}\right. \quad (3)$$

$$\left. - U_{\varphi,i}\frac{B_\varphi}{B_\theta}\left(U_{\theta,i} - \frac{T_i}{e_i B_\varphi}\frac{\partial \ln N_i^2 T_i}{\partial r}\right) + 1.90\frac{B_\varphi^2}{B_\theta^2}\left(U_{\theta,i} - 0.8\frac{T_i}{e_i B_\varphi}\frac{\partial \ln N_i^{1.6} T_i}{\partial r}\right)^2\right] - J_r B_\varphi,$$

where $\eta_{0,i}$ is the parallel viscosity coefficient.

Equations (2) and (3) have a two-time-scales-coupling between the poloidal and toroidal rotations and shows that the poloidal rotation velocity has a faster response time, $\tau_1 = \mu_{ex}^2 \tau_0$ [12, 17], where μ_{ex} is the expansion parameter to reduce the corrected Braginskii's equations. On a longer time scale, $\tau_0 \sim (\mu_{ex}^2 \nu_i)^{-1}$ however, if gyrostress tensor is properly taken into account, the poloidal and toroidal rotation velocities are strongly coupled. And, the poloidal rotation provides a further source mechanism for the toroidal rotation [16].

The temperature profile is prescribed and taken to be constant during the temporal evolution. The distribution along the spatial dimension can be approximated as a sum of special monotonic functions of the radial coordinate, ξ, [12]:

$$T(\xi) = T_s \sum_{i=1}^{n} A_i \left[- y_i(\xi)\right], \quad \text{where } y_i = \tanh\left(C_i + \xi/\mu_i\right) \quad (4)$$

where A_i, C_i, and μ_i are constants and T_s is the temperature at the separatrix. Functions y_i have the property $y_i' = \mu_i^{-1}(1-y_i^2)$ and $y_i'' = -2\mu_i^{-2} y_i (1-y_i^2)$. Therefore, the equations governing the motion of the plasma can be constructed as an autonomous system. By using the temperature values at the core side of the edge region and on the separatrix, we can get two equations for the two coefficients in the equation (4)

$$1 = \sum_{i=1}^{n} A_i \left[- \tanh(a_i)\right], \text{ and } T_c/T_s = 2\sum_{i=1}^{n} A_i \quad (5)$$

where T_c is the temperature at the inner side of the boundary. In order to reduce the computational expenses, here, temperature profile is taken simply as, $T(\xi) = 0.5 T_c \left[- \tanh\left(C_1 + \xi/\mu\right)\right]$, where $C_1 = \tanh^{-1}\left(- 2T_s/T_c\right)$. Therefore the steepness of the temperature profile is controlled by the parameter, μ. Hence, the derivative of the temperature can be expressed in terms of the temperature distribution instead of the radial coordinate as $T' = -(2/\mu)T\left[- (T_s/T_c)T\right]$, and $T'' = (2/\mu)^2 T\left[- (T_s/T_c)T\right]\left[- 2(T_s/T_c)T\right]$ [12, 19]. For different values of μ, some of the temperature profiles can be seen in FIG. 1. Note that as the μ decreases, i.e., as the profile steepens, the stored energy of the plasma increases.

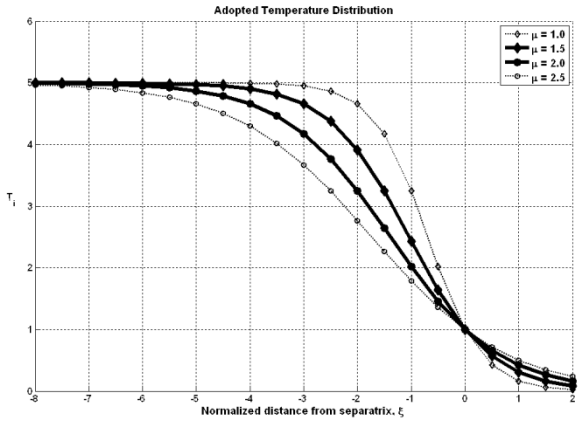

FIG. 1. Temperature profile. As the parameter μ, decreases, the profile become steeper. The distributions shown with solid thick lines have been used in velocity calculations.

3. Solution procedure

The long-time-scale behaviour of the poloidal and toroidal velocities is found to be governed by a (normalized) system of three quasilinear partial differential equations (6), where the space variable $\xi \equiv (r - r_s)/L_r$ is the normalized radial distance from the separatrix, L_r is the length scale of the temperature gradient and r_s is the radial location of the separatrix. Temperature is also nondimensionalized using the value at the separatrix, T_s. The toroidal (U_φ) and poloidal (U_θ) velocities are normalized by $\mu_{ex} c_i$ and $\mu_{ex}^2 c_i$, respectively. And the temporal evolution of the plasma is taken to be synchronized with the toroidal damping time, which is slower than the poloidal one by two orders [21]. The toroidal and poloidal rotation equations can be cast into a conservation form as follows:

$$\begin{bmatrix} 1 & 0 & 0 \\ 0 & F_{u_2} & 0 \\ 0 & 0 & F_{u_2}(\eta_2 F_{u_2} - G_{u_2} u_2 - G) \end{bmatrix} \frac{\partial \mathbf{u}}{\partial t} = \frac{\partial}{\partial \xi}\left(\left(\frac{1}{N_i}\frac{\partial u_3}{\partial \xi} + K_a u_1 + K_b \right) \begin{bmatrix} 0 \\ 1 \\ 1 \end{bmatrix} \right) + \left(\frac{1}{N_i}\frac{\partial u_3}{\partial \xi} + K_a u_1 + K_b \right) \begin{bmatrix} 1 \\ -F_{u_1} \\ F_{u_1}(\eta_2 F_{u_2} / \eta_2 F_{u_2} - G_{u_2} u_2 - G) - 1 \end{bmatrix} \tag{6}$$

The normalized toroidal and poloidal rotation velocities are expressed above by the u_1, u_2 components of the unknown vector **u**, respectively. The third component, u_3 is a nonlinear function of u_1, u_2, and $T(\xi)$, namely, $u_3 = u_3(\xi, u_1, u_2) = [\eta_2 F(\xi, u_1, u_2) - G(\xi, u_2) u_2]$, where

$$G = \eta_2 \frac{0.107\, q^2 (d \ln T / d\xi)}{1 + Q^2 / S^2} \ . \tag{7}$$

with

$$N_i \approx T^\gamma, \quad \eta_2 = 1.2 \times T^{\frac{4\gamma - 1}{2}}, \quad Q = 4[U_\theta - 0.625\,(2\gamma+1) dT/d\xi], \quad S = 4 \times 1.95\, T^{5/2-\gamma}. \tag{8}$$

and

$$F = \frac{\partial u_1}{\partial \xi} = -\frac{u_1^2}{2T} + u_1\left(\frac{u_2}{T} - \frac{d \ln N_i^2 T}{d\xi} \right) - 1.9T\left(\frac{u_2}{T} - 0.8 \frac{d \ln N_i^{1.6} T}{d\xi} \right)^2 + \frac{T^3}{N_i^2} \frac{u_2 + 1.833 (dT/d\xi) + \Delta}{0.45 (d \ln T / d\xi)} \left(1 + \frac{Q^2}{S^2} \right) \tag{9}$$

with the terms representing the charge exchange and radial current effects $K_a = -\nu_{CX}$, $K_B = J_r \cdot B_\theta$, respectively.

The quasilinear matrix equation (2) can be also rewritten as,

$$\mathbf{c}(\xi, t, \mathbf{u}, \frac{\partial \mathbf{u}}{\partial \xi}) \frac{\partial \mathbf{u}}{\partial t} = \frac{\partial}{\partial \xi}\left(\mathbf{f}\left(\xi, t, \mathbf{u}, \frac{\partial \mathbf{u}}{\partial \xi} \right)\right) + \mathbf{s}\left(\xi, t, \mathbf{u}, \frac{\partial \mathbf{u}}{\partial \xi} \right) \tag{10}$$

where

$$\mathbf{c} = \begin{bmatrix} 1 & 0 & 0 \\ 0 & F_{u_2} & 0 \\ 0 & 0 & F_{u_2}(\eta_2 F_{u_2} - G_{u_2} u_2 - G) \end{bmatrix}, \quad \mathbf{f} = \begin{bmatrix} 0 & 0 & 0 \\ 0 & 0 & 1/N_i \\ 0 & 0 & 1/N_i \end{bmatrix} \frac{\partial \mathbf{u}}{\partial \xi} + \begin{bmatrix} 0 & 0 & 0 \\ K_a & 0 & 0 \\ K_a & 0 & 0 \end{bmatrix} \mathbf{u} + \begin{bmatrix} 0 \\ K_b \\ K_b \end{bmatrix}, \text{ and}$$

$$\mathbf{s} = \begin{bmatrix} 0 & 0 & 1/N_i \\ 0 & 0 & -F_i/N_i \\ 0 & 0 & H/N_i \end{bmatrix} \frac{\partial \mathbf{u}}{\partial \xi} + \begin{bmatrix} 0 & 0 & 0 \\ -K_a F_{u_1} & 0 & 0 \\ K_a H & 0 & 0 \end{bmatrix} \mathbf{u} + \begin{bmatrix} K_b \\ -F_{u_1} K_b \\ H K_b \end{bmatrix},$$

where $H = F_{u_1}[\eta_2 F_{u_2} / (\eta_2 F_{u_2} - G_{u_2} u_2 - G) - 1]$.

The quasilinear system (10) can be numerically solved using a method provided by [22] for given initial $\mathbf{u}(\xi, t_0) = \mathbf{u_0}(\xi)$, and boundary conditions, at ξ=a or ξ=b for all t, of the form $\mathbf{p}(t, \xi, \mathbf{u}) + \mathbf{q}(t, \xi)\mathbf{f}(t, \xi, \mathbf{u}, \partial \mathbf{u} / \partial \xi) = 0$, where **p** and **f** are vectors and **q** is a diagonal matrix with elements that are either identically zero or never zero [22]. The thin edge region of a tokamak with large aspect ratio, as considered in this study, is taken as a slab model (m=0 in Ref. [22]). The steady state solutions of the system (2') have bifurcation behavior and richer structures especially when the temperature distribution becomes steeper, i.e. $\mu \to 0$ [12].

4. Results

By using a code to implement the solution procedure given in the previous section, we study the effect of the steepness of the temperature gradient. The radial coordinate is discretized by 300 stations and the 21 non-dimensional time steps have been taken to calculate the motion from t=0 to t=0.25. The temperature at core-side of the edge region is taken as 5 times of the temperature at the separatrix. In the solutions, Dirichlet-type boundary conditions are taken. The plasma is assumed to be at rest initially.

In the FIG. 2., and FIG. 3., the temporal evolution of toroidal and poloidal rotations of the plasma is presented, respectively, for μ=2, and μ=1.5 (steeper gradient) in the temperature distribution. In both figures, plasma gains momentum and accelerates in both toroidal and poloidal directions even without an external torque supplier in the neoclassical context. The driver of this motion is the gradient in the temperature distribution [16]. As the temperature gradient becomes steeper, i.e. as the stored energy of the plasma increases, it is seen that the maximum value of both toroidal and poloidal velocities increases.

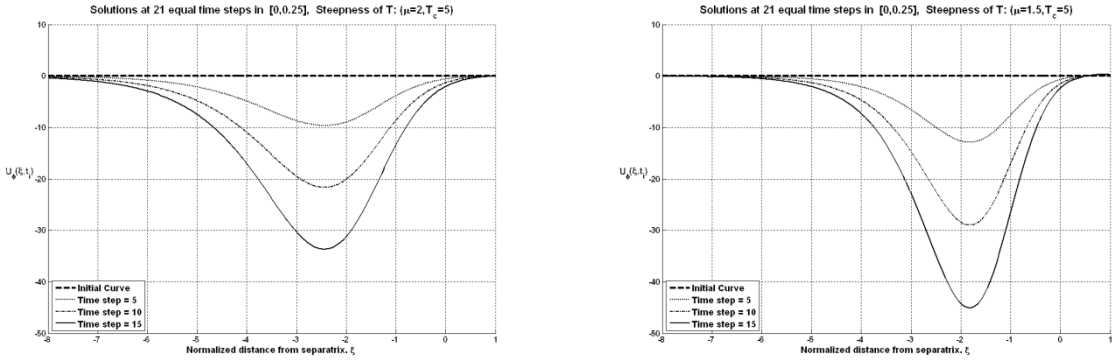

a) μ=2.0 *b) μ=1.5 (Steeper temperature profile)*

FIG. 2. Effect of the steep temperature profile on toroidal velocity, U_φ.

The maximum value of the poloidal rotation along the minor radius has a tendency to migrate through the core side, whereas toroidal rotation has no such behavior.

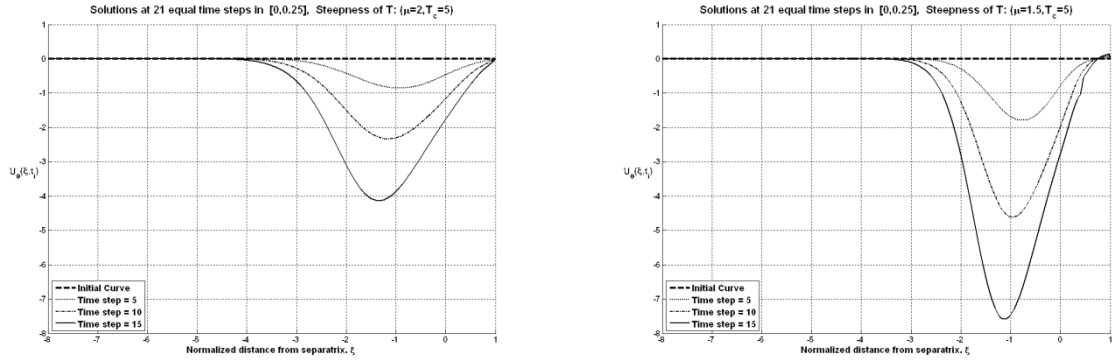

a) μ=2.0 *b) μ=1.5 (Steeper temperature profile)*

FIG. 3. Effect of the steep temperature profile on poloidal velocity, U_θ.

The electric field is calculated using radial momentum balance equation $E_r = B_\theta U_\varphi - B_\varphi U_\theta + (T_i / e_i)\,\partial \ln P_i / \partial r$ where P_i is the plasma pressure. In FIG. 4., non-dimensional electric field is shown with negative values along the edge region. Here, we note that the toroidal velocity term is dominating.

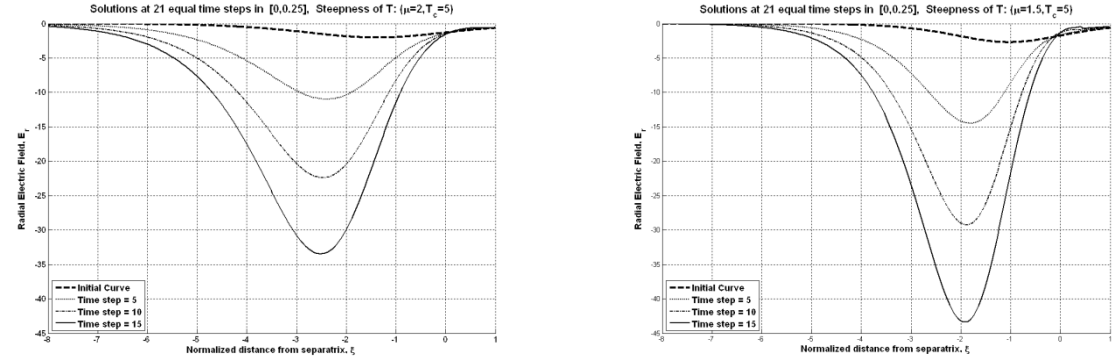

a) μ=2.0 *b) μ=1.5 (Steeper temperature profile)*

FIG. 4. Effect of the steep temperature profile on radial electric field, E_r.

Increasing the steepness of the temperature gradient also causes the plasma to have a reverse toroidal velocity around the separatrix side of the solution region. FIG. 5 is the blow-up view of the FIG. 2. Here, a small but persistent positive toroidal velocity for different steepness values is found. We have seen that steepening the gradient accentuates this behavior.

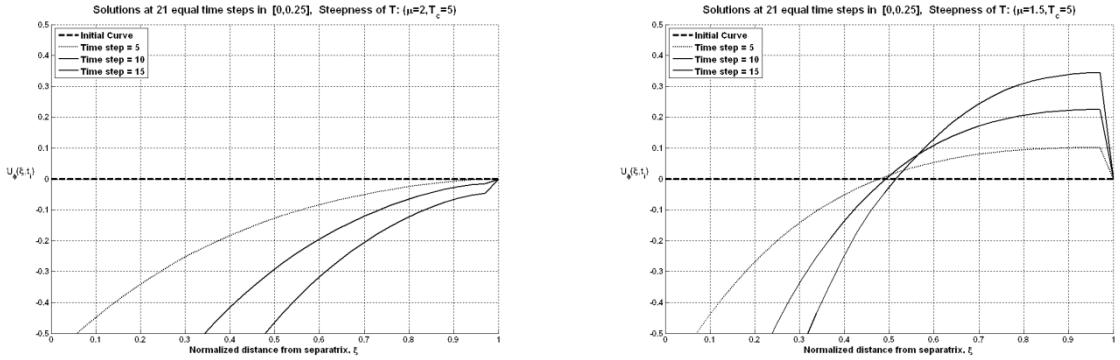

a) μ=2.0 *b) μ=1.5 (Steeper temperature profile)*

FIG. 5. Effect of the steep temperature profile on toroidal velocity, U_φ. Magnified view of the FIG. 2. Steeper gradient cause the plasma to rotate in reverse direction at the edge.

Changing the initial and boundary conditions in the core side of the plasma may cause the direction of the toroidal rotation to be reversed. It also makes the velocity distributions more complex. Examples of time dependent solutions of toroidal and poloidal velocities for moderately steep temperature profiles (μ=2) for non-zero boundary conditions are shown in FIG. 6. In this figure, spatial discretization is taken as the previous calculations. The equations are integrated for $t \in (0\ ,\ 2)$ interval with 20 non-dimensional time steps. For both toroidal and poloidal velocity, it is assumed a temperature like (tangent-hyperbolic) initial curve with $U_\varphi = 20$, $U_\theta = 5$ for $\xi = -8$ (i.e., core side) and $U_\varphi = -0.1$, $U_\theta = 0$ for $\xi = 1$ (i.e., outer side).

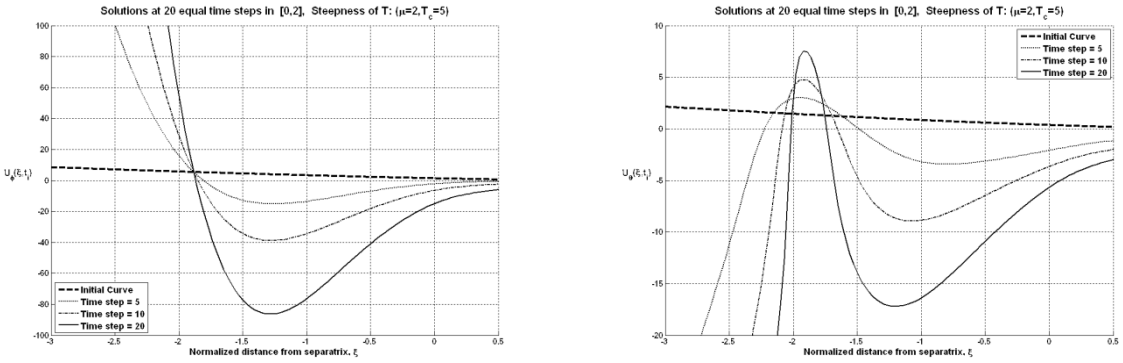

a) Toroidal velocity *b) Poloidal velocity*

FIG. 6. Initial and boundary value solutions for toroidal (a) and poloidal (b) rotation velocities with nonzero initial and boundary conditions.

We observe that for smaller μ values, i.e., for steeper temperature gradients, the velocities may have multi-valued solutions along the radius leading to possible mode transitions or instabilities. In such cases, adoption of a different numerical solution technique becomes necessary.

5. Conclusion

In this paper, flux-surface averaged equations governing the toroidal and poloidal motion of a collisional edge region of tokamak devices with circular cross-section and large aspect ratio were solved by numerical methods. Temperature profiles were assumed to be given and constant during the calculations. It is seen that both toroidal and poloidal rotation starts and grows even without external momentum source in initially non-rotating plasma as indicated by Ref. [16]. The terms in gyro-stress tensor for steep gradients acts as a toroidal momentum source in the neoclassical context. At the same time, the strong coupling between the parallel and toroidal momentum equations causes the plasma to rotate in the poloidal direction as well. Qualitative agreement between the results and the experiments for toroidal velocity and radial electric field encourages the quantitative comparisons in the future studies.

References

[1] RICE J.E., et. al. 2007 Nucl. Fusion **47** 1618
[2] STRINGER T.E. 1969 Phys.Rev. Lett. **22** 1770
[3] ROSENBLUTH M.N. and TAYLOR J.B. 1969 Phys. Rev. Lett. **23** 367
[4] HASSAM A. B. and KULSRUD R. M. 1978 Phys. Fluids **21** 2271
[5] COPPI B. 2002 Nucl. Fusion **42** 1
[6] SOLOMON W.M., et.al. 2009 Nucl. Fusion **49** 085005
[7] DIAMOND P.H., et. al. 2009 Nucl. Fusion **49** 045002.
[8] DEGRASSIE J. S. 2009 Nucl. Fusion **49** 085020
[9] DOYLE E.J., et. al. 2007 Nucl. Fusion **47** S18–S127
[10] RICE J.E., et. al., 2009 Nucl. Fusion **49** 025004
[11] ROSENBLUTH M.N., HINTON F.L. 1996 Nucl. Fusion **36** 55
[12] DAYBELGE U., YARIM C., and NICOLAI A. 2009 Nucl. Fusion **49** 115007
[13] BALESCU R., 1988 Transport Processes in Plasmas vol. 2, Neoclassical Transport (Amsterdam, North-Holland) p.659
[14] ROGISTER A. 1994 Phys. Plasmas **1** 619
[15] CLAASSEN H.A., and GERHAUSER H. 1999 Czech. J. Phys., **49** (Suppl. S3) 69
[16] CLAASSEN H.A., et. al. 2000 Phys. Plasmas **7** 3699
[17] DAYBELGE U., YARIM C., and NICOLAI A. 2004 Nucl. Fusion **44** 966
[18] NICOLAI A, DAYBELGE U, and YARIM C, 2004 Nucl. Fusion **44** S93
[19] MIKHAILOWSKII A.B. and TSYPIN V.S. 1984 Beitr. Plasmaphys. **24** 335.
[20] BRAGINSKII S.I. 1965 Reviews of Plasma Physics Vol.1 ed M.A. Leontovich (New York: Consultants Bureau) p. 205
[21] HIRSHMANN S.P. 1978 **18** 917
[22] SKEEL R.D. and BERZINS M. 1990 SIAM J. Sci. Stat. Comput. **11** 1